View metadata, citation and similar papers at core.ac.uk

brought to you by CORE

provided by Kyoto University Research Information Repository

KURENAI
Kyoto University Research Information Repository

KYOTO UNIVERSITY

Title	Mouse sperm undergo GPI-anchored protein release associated with lipid raft reorganization and acrosome reaction to acquire fertility.
Author(s)	Watanabe, Hitomi; Kondoh, Gen
Citation	Journal of cell science (2011), 124(15): 2573-2581
Issue Date	2011-08-01
URL	http://hdl.handle.net/2433/145976
Right	© The Company of Biologists Ltd 2011.
Type	Journal Article
Textversion	publisher

Kyoto University

Mouse sperm undergo GPI-anchored protein release associated with lipid raft reorganization and acrosome reaction to acquire fertility

Hitomi Watanabe and Gen Kondoh*

Laboratory of Animal Experiments for Regeneration, Institute for Frontier Medical Sciences, Kyoto University and CREST Program, Japan Science and Technology Society, 53 Syogoin-Kawahara-cho, Kyoto 606-8507, Japan

*Author for correspondence (kondohg@frontier.kyoto-u.ac.jp)

Accepted 28 March 2011
Journal of Cell Science 124, 2573-2581
© 2011. Published by The Company of Biologists Ltd
doi:10.1242/jcs.086967

Summary

Mammalian sperm undergo several maturation steps after leaving the testis to become competent for fertilization. Important changes occur in sperm within the female reproductive tract, although the molecular mechanisms underlying these processes remain unclear. To investigate sperm membrane remodeling upon sperm maturation, we developed transgenic mouse lines carrying glycosylphosphatidylinositol (GPI)-anchored enhanced green fluorescent protein (EGFP–GPI) and traced the fate of this fluorescent protein during the fertility-acquiring process in sperm in vitro and in vivo. When the GFP-labeled sperm were treated with compounds for promoting the acrosome reaction, EGFP–GPI was released from the sperm surface crosslinked with characteristic relocation of a lipid raft marker ganglioside GM1. Sperm ejaculated into the uterus strongly expressed EGFP–GPI in the head region, whereas a part of the oviductal sperm lost fluorescence in a manner that was dependent on the presence of angiotensin-converting enzyme (ACE). Moreover, sperm on the zona pellucida of eggs in the oviduct were all found to have low levels of GFP. These results suggest that sperm undergoing GPI-anchored protein release associated with reorganization of lipid rafts and the acrosome reaction acquire fertilization potential.

Key words: Sperm, Acrosome reaction, GM1, GPI-anchored protein, Lipid raft, Angiotensin-converting enzyme (ACE)

Introduction

The membranes of mammalian sperm undergo various modifications after leaving the testis in male and female reproductive tracts to acquire full competency to fertilize ova (Sullivan et al., 2005; Yanagimachi, 2009; Ikawa et al., 2010). One of the most important steps in this physiological change is capacitation, which occurs in the female reproductive tract and might be affected by humoral factors and the interaction between the sperm and the oviductal epithelium (Smith and Yanagimachi, 1990). During the capacitation process, it is reported that the sperm outer membrane undergoes cholesterol depletion, followed by downstream signaling processes such as protein tyrosine phosphorylation (Visconti et al., 1995; Visconti et al., 1999; Travis and Kopf, 2002; Bailey, 2010). Because cholesterol is a major component of lipid rafts (Jacobson et al., 2007; Simons and Toomre, 2000), its efflux might also change membrane fluidity and/or induce rearrangement of lipid rafts (Davis, 1981; Nixon et al., 2008), although other molecular mechanisms involved in capacitation remain to be characterized. Several biological processes seem to be associated with the lipid microdomain (Mishra and Joshi, 2007). Numerous sperm surface proteins are components of this structure and some are directly involved in sperm–zona-pellucida (ZP) binding (Nixon et al., 2008); however, the biological implications of this structure in fertilization have yet to be determined. Another important step is the acrosome reaction (Wassarman and Litscher, 2001; Clark and Dell, 2006; Wassarman and Litscher, 2008; Suarez, 2008). The acrosome is a Golgi-derived organelle that overlies the sperm nucleus in the apical region of the head. It consists of a continuous membrane, called the inner and outer acrosome membrane. Upon the acrosome reaction, the outer acrosomal membrane and the plasma membrane of sperm fuse, forming multiple hybrid membrane vesicles, following exposure of inner acrosomal membrane and release of acrosomal ingredients. ZP binding of the sperm is a trigger of the acrosome reaction in vivo, and this process can be experimentally prompted by treating sperm with a calcium ionophore to facilitate Ca^{2+} influx (Costello et al., 2009). Sperm that have completed the acrosome reaction can exclusively penetrate the ZP and fuse with the egg plasma membrane.

It is well known that glycosylphosphatidylinositol (GPI)-anchored proteins (GPI-APs) are a major component of lipid rafts (Varma and Mayor, 1998). To monitor the fates of GPI-APs, as well as lipid rafts, in vivo, we previously developed GPI-anchored enhanced green fluorescent protein (EGFP–GPI) and examined the localization and release of GPI-APs in various tissues (Kondoh et al., 1999). In further studies, we and others showed that the release of GPI-APs from the sperm membrane is crucial for male fertility, particularly for the sperm–egg binding step (Kondoh et al., 2005; Ueda et al., 2007).

Izumo1 is a transmembrane protein that is involved in sperm–egg fusion (Inoue et al., 2005), which is also located in lipid rafts (Nixon et al., 2008) and is an indicator of the acrosome reaction (Fujiwara et al., 2010). First, we discovered a linkage between GPI-AP release and ganglioside GM1 relocation. GM1 is a characteristic component and reliable biomarker of lipid rafts. Other studies showed that it dynamically moves with methyl-β-cyclodextrin (M-β-CD) treatment in the mouse sperm membrane (Buttke et al., 2006; Selvaraj et al., 2007). Here, we found that M-

β-CD induces both GPI-AP release and GM1 relocation. The pharmacological effect of M-β-CD is to capture cholesterol, thus it is believed that its main functions in the sperm fertility acquisition process are to facilitate cholesterol efflux and to induce capacitation (Takeo et al., 2008). By monitoring relocation of Izumo1, we also found that M-β-CD can induce the acrosome reaction.

Addition of bovine serum albumin (BSA) alone could induce neither GPI-AP release nor GM relocation, but could do so following treatment with the calcium ionophore A23187. We thus conclude that lipid raft movement occurs upon the acrosome reaction, rather than upon capacitation. Our observations here suggest a molecular process by which sperm acquire fertility.

Results

Production of EGFP(K268Q)-GPI transgenic mice

We previously developed an EGFP–GPI reporter protein to follow the fate of GPI in vivo (Kondoh et al., 1999). However, the original construct encoded a lysine residue adjacent to the GPI attachment site that seemed to be a target for serine proteases. To reduce the possibility of nonspecific cleavage by proteases, we replaced the lysine at residue 268 with glutamine (supplementary material Fig. S1A) and designated the protein EGFP(K268Q)-GPI. Expression of this construct in cultured cells revealed GFP on the cell surface and on the Golgi complex (supplementary material Fig. S1B). Treatment with the phosphatidylinositol-specific phospholipase C (PI-PLC) virtually abrogated the cell-surface signal, confirming that the protein is GPI anchored.

We next developed transgenic mouse lines carrying the EGFP(K268Q)-GPI sequence to examine the fate of GPI-anchored proteins in vivo. Three transgenic founders were obtained by injecting the transgene into one-cell embryos of the C57BL/6 genetic background, with two founders showing protein expression in the sperm head and cytoplasmic droplet (supplementary material Fig. S1C). Transgenic line 2 showed relatively high expression and thus was selected for further analyses. Male mice of this line showed normal fertility rate (mean no. of litters ± s.d.: 6.83±2.1, *n*=6), which was comparable to that of C57BL/6 non-transgenic controls (6–7 newborns per litter). The transgene was inherited by their descendants in accordance with the expected Mendelian frequencies.

EGFP–GPI release and GM1 relocation upon treatment with M-β-CD

To induce sperm maturation in vitro, M-β-CD or BSA was used in this study. Both compounds bind cholesterol and facilitate its depletion from the cell membrane. First, sperm were collected from the epididymis of transgenic mice and incubated in HTF-PVA with or without 0.45 mM M-β-CD. This concentration of M-β-CD is reported to induce capacitation in vitro (Visconti et al., 1999). Indeed, sperm faithfully acquired fertility in our examinations (Fig. 1A), implying that this treatment is not harmful but is preferable for in vitro fertilization (Fig. 1B). Moreover, fertilized eggs from HTF-PVA insemination were transferred to pseudo-pregnant females and normal pups were obtained in significant numbers (82 newborns after 193 embryos transferred). Next, we investigated the fate of EGFP(K268Q)-GPI in the sperm. Fluorescence microscopy revealed that the EGFP(K268Q)-GPI expression in the sperm head was distributed in one of the two patterns: ‘bright’ and ‘shed’ (Fig. 2A). Fluorescence in the sperm tail was deemed nonspecific autofluorescence, which also appeared in non-transgenic controls. As indicated in Fig. 2B, sperm showing the shed pattern of EGFP(K268Q)-GPI increased in frequency in a time-dependent manner in the presence of M-β-CD. A subpopulation of the GFP-less sperm was also observed in M-β-CD-free incubations, indicating spontaneous GFP loss for an unknown reason. The ganglioside GM1, which is a characteristic component of lipid rafts in the plasma membrane, can be specifically visualized using cholera toxin B subunit (CTB). We observed three patterns of GM1 localization after staining with Alexa-Fluor-594-labeled CTB: ‘hazy’, ‘apical ridge’ and ‘entire head’ (Fig. 2A). These patterns of staining could be related to the EGFP(K268Q)-GPI localization. As indicated in Fig. 2C, sperm with the entire head pattern appeared at a similar time course and rate as seen with the shedding of EGFP(K268Q)-GPI. The hazy pattern was only observed in bright sperm, for which the most predominant pattern of GM1 staining was apical ridge pattern. By contrast, almost all of the shed sperm showed the entire head pattern (Fig. 2D). These observations suggested that shedding of EGFP(K268Q)-GPI is linked to the relocation of GM1.

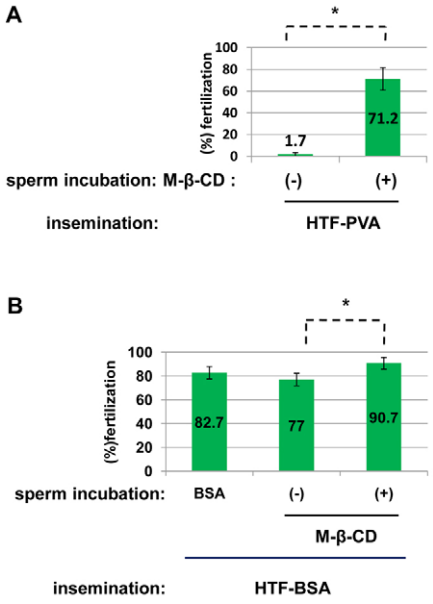

Fig. 1. In vitro fertility of sperm incubated with M-β-CD. Epididymal sperm were incubated in HTF-M-β-CD for 120 minutes and then inseminated with cumulus-positive oocytes in HTF-PVA (**A**) or HTF-BSA (**B**). Sperm incubated without M-β-CD were also fertile when the insemination was performed in HTF-BSA, under conditions that might induce capacitation. Efficiency of in vitro fertilization is indicated as percentage fertilization. Three independent experiments were performed for each incubation. Number of eggs examined: (A) M-β-CD–, *n*=354; M-β-CD+, *n*=370; (B) BSA, *n*=367; M-β-CD–, *n*=306; M-β-CD+, *n*=246. Results are means ± s.d. *$P<0.05$ (Student’s *t*-test).

Moreover, the release of GPI-AP was not specific for EGFP(K268Q)-GPI. As shown in Fig. 3, endogenous GPI-APs, such as Hyal5 and Prss21, were released in the presence of M-β-CD at the same time, whereas another GPI-AP, Spam1, was readily released in an M-β-CD-independent manner. It is notable that all such secreted proteins detected in the culture supernatants were comparable in molecular size to the membrane-bound form. By contrast, transmembrane proteins such as Adam2, Adam3, Izumo1 and angiotensin-converting enzyme (ACE), or the endoplasmic reticulum-linked protein Ces3 were not necessarily secreted following M-β-CD treatment.

Journal of Cell Science

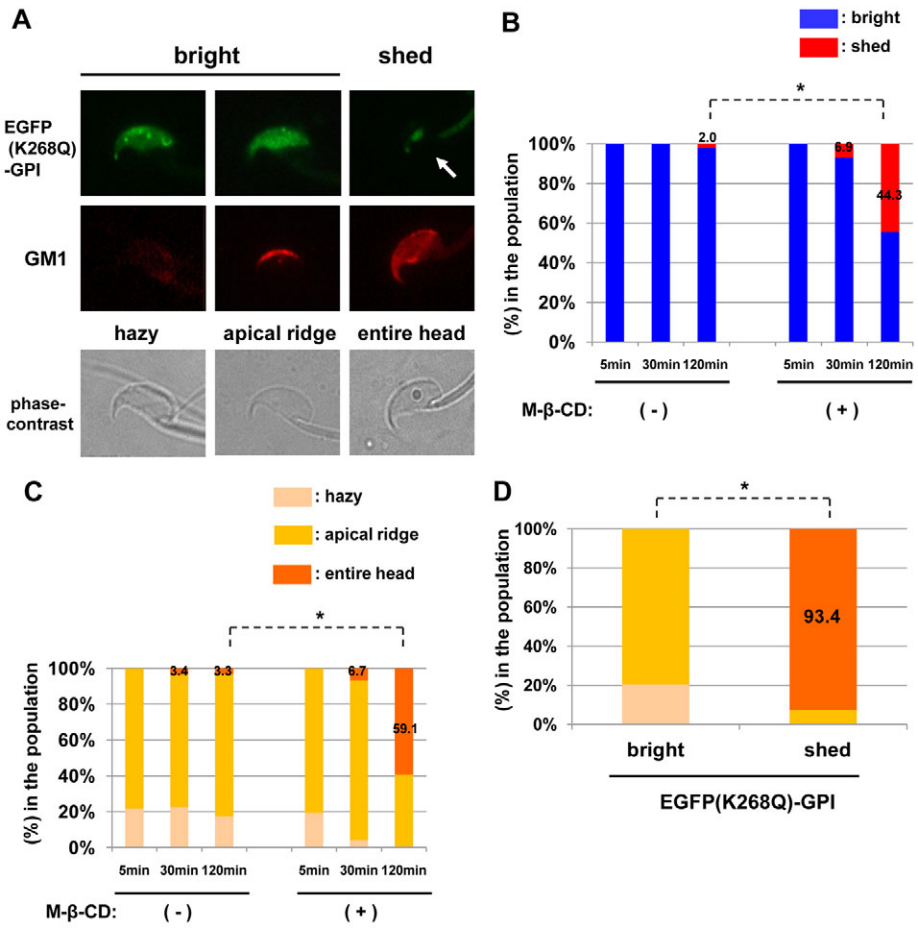

Fig. 2. Fate of EGFP(K268Q)-GPI and GM1 upon M-β-CD treatment. (**A**) EGFP(K268Q)-GPI shedding relative to GM1 reorganization. Expression patterns of EGFP(K268Q)-GPI in the transgenic sperm heads are displayed in the top panels, designated as bright and shed. Weak but apparent GFP fluorescence remained in the central portion of the sperm head even after shedding (arrow). The fluorescence in the sperm tails was nonspecific autofluorescence, which was also detected in nontransgenic controls. GM1 was localized by staining with Alexa-Fluor-594-conjugated CTB (middle panels) and the patterns were designated as hazy, apical ridge and entire head. The bottom panels represent the phase-contrast views. (**B**) Fate of epididymal sperm incubated with M-β-CD. Sperm collected from the epididymis were incubated in HTF-PVA medium with or without M-β-CD for the indicated times. Sperm classified with regard to the dual patterns are indicated by their proportion in the population examined. Number of sperm examined: M-β-CD– 5 minutes, *n*=352; 30 minutes, *n*=355; 120 minutes, *n*=346; M-β-CD+ 5 minutes, *n*=349; 30 minutes, *n*=345; 120 minutes, *n*=406. Data from three independent experiments were accumulated. Percentage of shed sperm is indicated. (**C**) GM1 staining patterns. Sperm were cultured as in B and stained with Alexa-Fluor-594-conjugated CTB. Number of sperm examined: M-β-CD– 5 minutes, *n*=381; 30 minutes, *n*=373; 120 minutes, *n*=363; M-β-CD+ 5 minutes, *n*=391; 30 minutes, *n*=459; 120 minutes, *n*=544. Data from three independent experiments were accumulated. Percentage of entire head sperm is indicated. (**D**) GM1 staining patterns combined with EGFP(K268Q)-GPI fates. Sperm were cultured as in B for 120 minutes and stained with Alexa-Fluor-594-conjugated CTB. Number of sperm examined: bright, *n*=189; shed, *n*=153. Data from three independent experiments were accumulated. Percentage of entire head sperm is indicated. *$P<0.05$ (Student's *t*-test).

EGFP–GPI release and GM1 relocation is associated with the acrosome reaction

Next, we examined shedding of EGFP(K268Q)-GPI and GM1 relocation in sperm using BSA. However, we could observe neither significant EGFP(K268Q)-GPI shedding nor GM1 relocation, suggesting that BSA has a different method for inducing sperm fertility in vitro (Fig. 4A,B). It is well known that BSA alone faithfully induces capacitation but not the acrosome reaction (Fig. 4C). Thus, we treated BSA-incubated sperm with the calcium ionophore A23187 to promote the acrosome reaction. The acrosome reaction was detected by relocation of Izumo1, which is distributed throughout the entire head when sperm undergo the acrosome reaction (Okabe et al., 1987; Fujiwara et al., 2010; Ikawa et al., 2010). A23187 treatment promoted the acrosome reaction (Fig. 4F). Because A23187 alone could not induce the acrosome reaction (supplementary material Fig. S2), it was confirmed that the acrosome reaction here is due to an effect of BSA. At the same time, shedding of EGFP(K268Q)-GPI and relocation of GM1 was observed (Fig. 4D,E). The bright sperm also showed significant labeling of GM1 in an 'entire head' pattern, suggesting that movement of GM1 precedes GPI-AP release and the acrosome reaction (Fig. 4G,H). These observations prompted us to examine the state of the acrosome in M-β-CD-treated sperm. As shown in Fig. 5A,B, Izumo1 relocated upon M-β-CD treatment, indicating that M-β-CD can efficiently induce the acrosome reaction, as well as capacitation. This effect of M-β-CD was confirmed by treating Acrosin–EGFP transgenic sperm with the compound (supplementary material Fig. S3). These sperm show dispersion of Acrosin–EGFP fusion protein upon the acrosome reaction and become GFP negative (Nakanishi et al., 1999). Furthermore, 90%

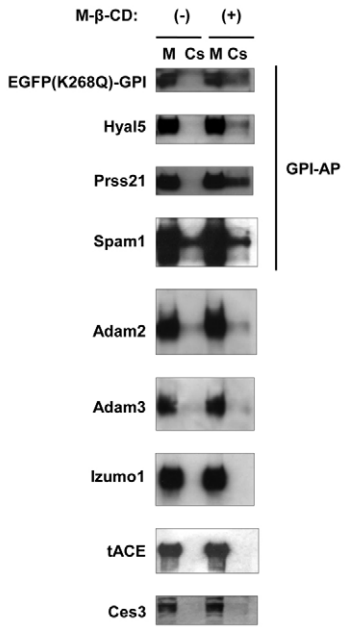

Fig. 3. Distribution of sperm membrane proteins upon M-β-CD treatment. Epididymal sperm were incubated as in Fig. 2B for 120 minutes. Membrane fractions (M) and culture supernatants (Cs) of EGFP(K268Q)-GPI sperm were subjected to immunoblotting using 10 µg of protein, which represented 1/6 of the total protein in membrane fractions and 1/36 of the total protein in culture supernatants. GPI-APs: EGFP(K268Q)-GPI, Hyal5, Prss21 and Spam1. Transmembrane proteins: Adam2, Adam3, Izumo1 and tACE. Endoplasmic reticulum-associated protein: Ces3.

of EGFP(K268Q)-GPI shed sperm underwent the acrosome reaction (Fig. 5C). These observations strongly suggest that release of GPI–AP and lipid raft movement occur during the acrosome reaction, rather than during capacitation.

Sperm bound to ZP have low levels of GFP and relocated GM1

We next examined the fate of EGFP(K268Q)-GPI in vivo. Because GM1 and Izumo1 always colocalize and move in similar manners (supplementary material Fig. S4), the fate of lipid rafts and the degree of completed acrosome reaction was followed by GM1 staining in in vivo studies. First, we observed the expression of EGFP(K268Q)-GPI in sperm ejaculated into the uterus and in those that migrated to the oviducts. Almost all uterine sperm showed a bright pattern (Fig. 6A). By contrast, about 40% of the sperm in the oviducts showed the 'shed' pattern. The GM1 patterns were also examined, and we found that the proportion of sperm labeled over the 'entire head' with GM1 correlated with the 'shed' sperm in the oviduct (Fig. 6B), which corresponds to the findings of our in vitro experiments.

To determine whether uterine sperm are capable of shedding, they were collected and incubated in the presence of M-β-CD, and then examined for EGFP(K268Q)-GPI expression by fluorescence microscopy. The uterine sperm acquired competency for shedding upon M-β-CD treatment (Fig. 6C), indicating that sperm at this location possess the potential for shedding and that the limited number of shed sperm in the oviducts might reflect the environmental capacity to induce sperm fertility. Here, we found again that the number of 'entire head' GM1 sperm increased only when the EGFP–GPI shedding was induced (Fig. 6D).

Previously, sperm from *Ace*-knockout mice were reported to show phenotypes such as inability to migrate into the oviduct and ZP-binding deficiencies (Hagaman et al., 1998). We also reported that ACE can contribute to form sperm–ZP binding ability through its GPI-AP releasing activity (GPIase) (Kondoh et al., 2005). Therefore, in the present study, we tried to confirm the contribution of ACE to the release of GPI-AP. We also prepared *Ace*-knockout mice carrying EGFP(K268Q)-GPI and examined uterine sperm, which are destined to fail in migrating into the oviduct. When the recovered sperm were treated with M-β-CD, more than 90% retained a bright appearance (Fig. 6E), indicating that shedding of EGFP(K268Q)-GPI is suppressed by ACE deficiency. The localization of GM1 also showed less transition to the entire head pattern (Fig. 6F). These observations suggest that ACE governs both GPI-AP release and lipid raft movement upon the acrosome reaction.

To examine our theory regarding the location for fertilization, eggs surrounded by cumulus cells were collected from the ampullae of mated female oviducts to assess sperm penetrating the cumulus layer or binding to the ZP of the egg. All sperm that bound to the ZP showed the shed pattern of EGFP(K268Q)-GPI and the entire head pattern for GM1 (Fig. 6G–I). Similar results were observed in sperm with in vitro fertilization (Fig. 6J,K). These results strongly suggest that sperm that have undergone GPI-AP release and GM1 relocation exclusively acquire fertility in vivo.

Discussion

In this study, we compared the effects of two compounds, M-β-CD and BSA, for inducing sperm maturation in vitro and revealed that the release of GPI-APs and lipid raft movement occur upon the acrosome reaction. We found that M-β-CD can induce the acrosome reaction, as well as capacitation.

Ace-knockout sperm collected from the uterus showed less GM1 relocation, as well as low GPI-AP release, after M-β-CD treatment. These observations suggest that ACE is involved in the acrosome reaction. In a previous report, ACE-knockout sperm showed normal acrosome reactions induced by treatment with BSA and A23187 (Hagaman et al., 1998). The discrepancy between these observations and ours might be due to a difference in the pharmacological effects of the drugs used. M-β-CD facilitates cholesterol efflux from the sperm membrane and causes capacitation followed by the acrosome reaction, affecting the early step of sperm maturation. By contrast, A23187 facilitates Ca^{2+} influx and completes acrosome exocytosis, which is a late step. Thus, these observations might explain why ACE participates in the capacitation and/or early step of acrosome reaction, but not in the late step.

As shown in our previous study, disruption of lipid rafts is required for detecting ACE GPIase activity on the cell surface (Kondoh et al., 2005), suggesting that the lipid raft structure protects GPI-APs from release by ACE. Upon capacitation followed by the acrosome reaction, cholesterol efflux from the sperm membrane is facilitated, which results in lipid raft movement and possibly loosening of the structure; thus GPI-APs suffer from ACE attack.

Recently, it was reported that sperm–ZP binding is not sufficient for inducing acrosome exocytosis, but it requires cleavage of the ZP2 protein (Baibakov et al., 2007). In this study, the authors monitored the acrosome reaction by dispersion of an Acrosin–GFP fusion protein, which took more than 2 hours to complete. However,

Journal of Cell Science

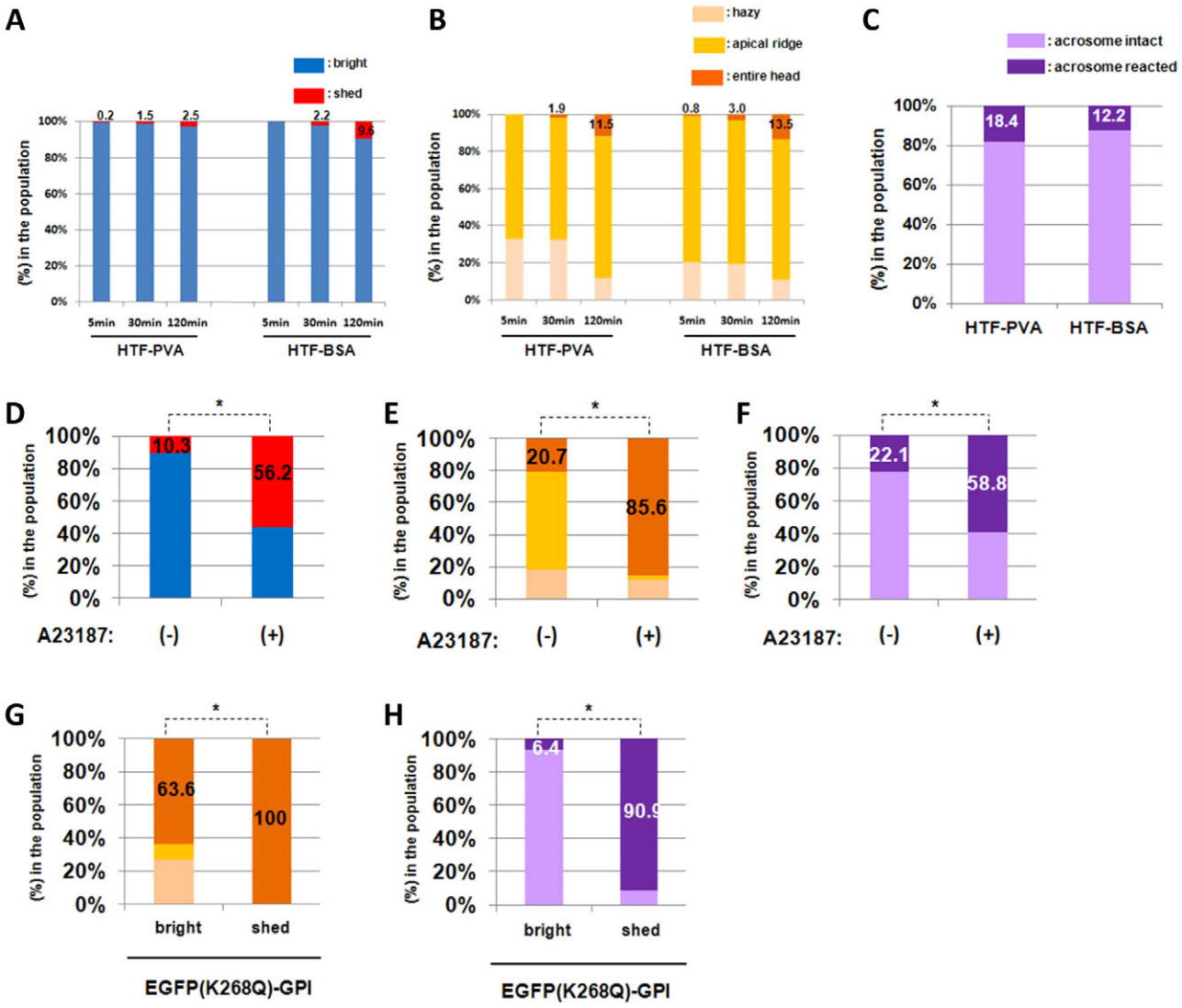

Fig. 4. EGFP(K268Q)-GPI release and GM1 relocation is associated with acrosome reaction. (**A**) EGFP(K268Q)-GPI fate of cultured epididymal sperm. Sperm collected from the epididymis were cultured in HTF-PVA or HTF-BSA for the indicated times. Sperm classified with regard to the dual patterns are indicated by their proportion in the population examined. Number of sperm examined: HTF-PVA 5 minutes, *n*=372; 30 minutes, *n*=326; 120 minutes, *n*=355; and HTF-BSA 5 minutes, *n*=341; 30 minutes, *n*=352; 120 minutes, *n*=373. Data from three independent experiments were accumulated. Percentage shed sperm is indicated. (**B**) GM1 staining patterns. Sperm were cultured as in A and stained with Alexa-Fluor-594-conjugated CTB. Number of sperm examined: HTF-PVA 5 minutes, *n*=407; 30 minutes, *n*=258; 120 minutes, *n*=365; and HTF-BSA 5 minutes, *n*=348; 30 minutes, *n*=359; 120 minutes, *n*=390. Data from three independent experiments were accumulated. Percentage entire head sperm is indicated. (**C**) Izumo1 immunostaining to evaluate acrosome status. Sperm that had undergone acrosome reaction were stained as entire head pattern, whereas sperm without acrosome reaction were stained as acrosomal cap pattern (see Fig. 5). Sperm collected from the epididymis were incubated in HTF-PVA or HTF-BSA medium for 120 minutes. Sperm classified with regard to the dual patterns are indicated by their proportion in the population examined. Number of sperm examined: M-β-CD–, *n*=444; M-β-CD+, *n*=376. Data from three independent experiments were accumulated. Percentage acrosome-reacted sperm is indicated. (**D**) EGFP(K268Q)-GPI status with calcium ionophore treatment. Epididymal sperm were pre-incubated in HTF-BSA for 120 minutes and then further incubated in HTF-BSA containing A23187 for 60 minutes. Sperm classified with regard to the dual patterns are indicated by their proportion in the population examined. Number of sperm examined: A23187–, *n*=318; A23187+, *n*=354. Data from three independent experiments were accumulated. Percentage shed sperm is indicated. (**E**) GM1 status with calcium ionophore treatment. Number of sperm examined: A23187–, *n*=308; A23187+, *n*=313. Data from three independent experiments were accumulated. Percentage entire head sperm is indicated. (**F**) Izumo1 immunostaining after treatment with a calcium ionophore. Acrosome-reacted sperm were stained as entire head pattern and acrosome-intact sperm as acrosomal cap pattern (see Fig. 5). Number of sperm examined: A23187–, *n*=434; A23187+, *n*=425. Data from three independent experiments were accumulated. Percentage acrosome-reacted sperm is indicated. (**G**) GM1 staining patterns combined with EGFP(K268Q)-GPI fates. Number of sperm examined: bright, *n*=154; shed, *n*=162. Data from three independent experiments were accumulated. Percentage entire head sperm is indicated. (**H**) Izumo1 staining patterns combined with EGFP(K268Q)-GPI fates. Number of sperm examined: bright, *n*=156; shed, *n*=155. Data from three independent experiments were accumulated. Percentage acrosome-reacted sperm is indicated. *P<0.05 (Student's *t*-test).

we observed that all sperm bound to ZP were negative for Acrosin–EGFP, as well as relocated GM1 (supplementary material Fig. S5). The difference might be due to the compound used. They pre-incubated sperm with BSA-containing medium before IVF, whereas we used M-β-CD. Because BSA can capacitate sperm but not induce the acrosome reaction (Fig. 4), the acrosome reaction only

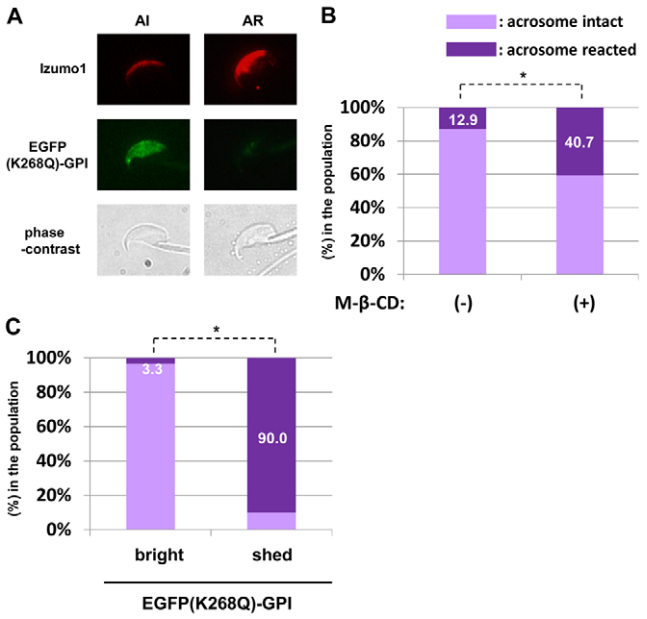

Fig. 5. Induction of acrosome reaction by M-β-CD. (**A**) Acrosome status of sperm. Expression patterns of Izumo1 in the transgenic sperm heads are displayed, designated as acrosomal cap (acrosome intact, AI) and entire head (acrosome reacted, AR) patterns. (**B**) Acrosome reaction upon M-β-CD treatment. Sperm collected from the epididymis were incubated in HTF-PVA medium with or without M-β-CD for 120 minutes. Sperm classified with regard to the dual patterns are indicated by their proportion in the population examined. Number of sperm examined: M-β-CD–, *n*=364; M-β-CD+, *n*=461. Data from three independent experiments were accumulated. Percentage acrosome-reacted sperm is indicated. (**C**) Acrosome status combined with EGFP(K268Q)-GPI fates. Number of sperm examined: bright, *n*=211; shed, *n*=212. Data from three independent experiments were accumulated. Percentage acrosome-reacted sperm is indicated. **P*<0.05 (Student's *t*-test).

starts upon ZP binding; this allows more time for sperm to be GFP negative. By contrast, M-β-CD induces the acrosome reaction as well as capacitation (Fig. 5 and supplementary material Fig. S3). Thus, all M-β-CD-treated sperm bound to ZP are already acrosome-reacted and are GFP negative and have relocated GM1.

The movement of GM1 upon M-β-CD treatment was reported previously (Nixon et al., 2008; Selvaraj et al., 2007). Recently, a precise study was performed on boar sperm (Jones et al., 2010). It was observed that GM1 was first accumulated on apical ridge and then diffused to the equatorial region. Although the equatorial CTB staining pattern was different between mouse and boar sperm, the paths of GM1 movement seemed to be similar. The meaning of this movement should be elucidated further.

Only those sperm that had shed GPI-APs bound to eggs. We showed previously that ACE has GPIase activity contributing to sperm–ZP binding (Kondoh et al., 2005). Fuchs and colleagues reported that dipeptidase activity of testicular ACE (tACE) is required for sperm–ZP binding (Fuchs et al., 2005). Thereafter, we reported that dipeptidase activity of tACE is functional in the epididymis (Deguchi et al., 2007). In addition, Shum and co-workers have shown that angiotensin II, a product of ACE dipeptidase action, regulates the distribution of proton channels in the epididymal epithelium and contributes to the pH homeostasis of the epididymal fluids (Shum et al., 2008). Because the pH of the epididymis is maintained at a low level and the GPIase activity of ACE prefers a low pH (pH 6.5 for maximum activity), it is possible that the dideptidase activity of ACE indirectly supports its GPIase activity by maintaining a suitable pH. In this scheme, the GPI-AP status of the epididymal sperm membrane might be regulated by both ACE activities.

Ace- and *Pgap1* (post-GPI attachment to proteins 1)-knockout mice reportedly show phenotypes consistent with male infertility, such as sperm uterotubular migration and ZP-binding deficiencies (Kondoh et al., 2005; Ueda et al., 2007). In these mice, sperm retained GPI-APs in their membranes. These mutually exclusive findings – GPI-AP retention in the sperm membrane linked with insufficiency of sperm–ZP binding in two independent knockout mice, and GPI-AP shed in all sperm bound to the ZP – strongly suggest that the release of some GPI-APs from the sperm membrane is crucial for sperm to acquire fertility in the female reproductive tract. More than 20 years ago, Yanagimachi speculated that capacitation is a process for gradual removal of coating material to expose sperm receptors for binding to an egg (Yanagimachi, 1988). Our findings on GPI-AP release might support this, but further elucidation is required.

Materials and Methods

Development of K268Q-GPI–EGFP

K268Q-converted EGFP–GPI (EGFP(K268Q)-GPI) was developed as described previously with slight modification (Kondoh et al., 2009). Briefly, a mutated product was developed by amplifying the left and right fragments using fixed primers specific for regions located outside of the coding region and back-to-back primers carrying mutations. The PCR products were generated by *Pfx* polymerase, which does not add a nucleotide at the 5′ end. Finally, the CAAG ubiquitously expressing vector, which carries a strong and broad driving element containing the cytomegalovirus immediate-early enhancer and chicken β-actin promoter (Niwa et al., 1991), cleaved with *Eco*RI followed by blunt-ending, was ligated with the respective PCR products. All ligated constructs were sequenced to verify the introduced mutations and to exclude PCR-related errors. Supplementary material Table S1 lists the primers used.

Expression of EGFP(K268Q)-GPI in culture cells and PI-PLC treatment

The EGFP(K268Q)-GPI vector constructed above was transfected into CHO cells, and then cells expressing EGFP(K268Q)-GPI were selected by fluorescence-activated cell sorting (FACS). These cells were treated with 1.0 IU/ml of phosphatidylinositol-specific phospholipase C (Molecular Probes, Eugene, OR) in OPTI-CHO medium (Invitrogen, Carlsbad, CA) for 1 hour at 37°C, washed with phosphate-buffered saline (PBS) and observed under a fluorescent microscope (Olympus, Tokyo, Japan).

Development of EGFP(K268Q)-GPI transgenic mice and animal maintenance

The *CAAG-EGFP K268QGPI* transgene was injected into C57BL/6J one-cell embryos and transgenic lines were maintained by mating on the isogenic background. Transgenic founders were obtained by PCR screening of siblings using tail DNA as a template and primers, 5′-TTCTTCAAGGACGACGGCAACTACAAGACC-3′ and 5′-GTCACGAACTCCAGCAGGACCATGTGATCG-3′. The same PCR screening was also used for selecting Acrosin–EGFP transgenic mice. *Ace*-knockout mice (JR#002679) were purchased from the Jackson Laboratory (Bar Harbor, ME) and screened by PCR using primers, 5′-CTTGACGAGTTCTTCTGAGG-3′, 5′-AGAAAAGCACGGAGGTATCC-3′ and 5′-ACTGCCCGGTCCAGGTTCTG-3′.

Ace-knockout mice carrying EGFP(K268Q)-GPI were developed by mating mice heterozygous for *Ace*-disrupted allele with the line 2 EGFP(K268Q)-GPI transgenic mice. All animal experiments were approved by the Animal Experiment Committees of the Institute for Frontier Medical Sciences and Kyoto University.

Sperm collection, incubation, GM1 staining and observation

We used the human tubular fluid (HTF)-base medium (101.61 mM NaCl, 4.69 mM KCl, 0.2 mM $MgSO_4$, 0.4 mM KH_2PO_4, 6.42 mM $CaCl_2$, 25 mM $NaHCO_3$, 2.77 mM glucose, 3.4 μg/ml sodium lactate, 0.34 mM sodium pyruvate, 0.2 mM penicillin G sodium salt, 0.03 mM streptomycin and 0.4 μl of 0.5% Phenol Red) supplemented with 1 mg/ml polyvinyl alcohol (PVA) (Sigma, St Louis, MO) (HTF-PVA) for sperm incubation and in vitro fertilization. To induce in vitro fertility, 0.45 mM methyl-β-cyclodextrin (Sigma) was added to the HTF-PVA (HTF-PVA-M-β-CD). HTF-base medium containing 4 mg/ml bovine serum albumin (BSA) (Sigma) was also used for sperm incubation (HTF-BSA). Sperm from the cauda epididymis were incubated in HTF-PVA, HTF-PVA-M-β-CD, or HTF-BSA for the indicated times. More than 90% of sperm were motile even after 2 hours of incubation. After incubation, 10 mM EDTA was added to the samples and they were placed on ice to stop further reaction

Journal of Cell Science

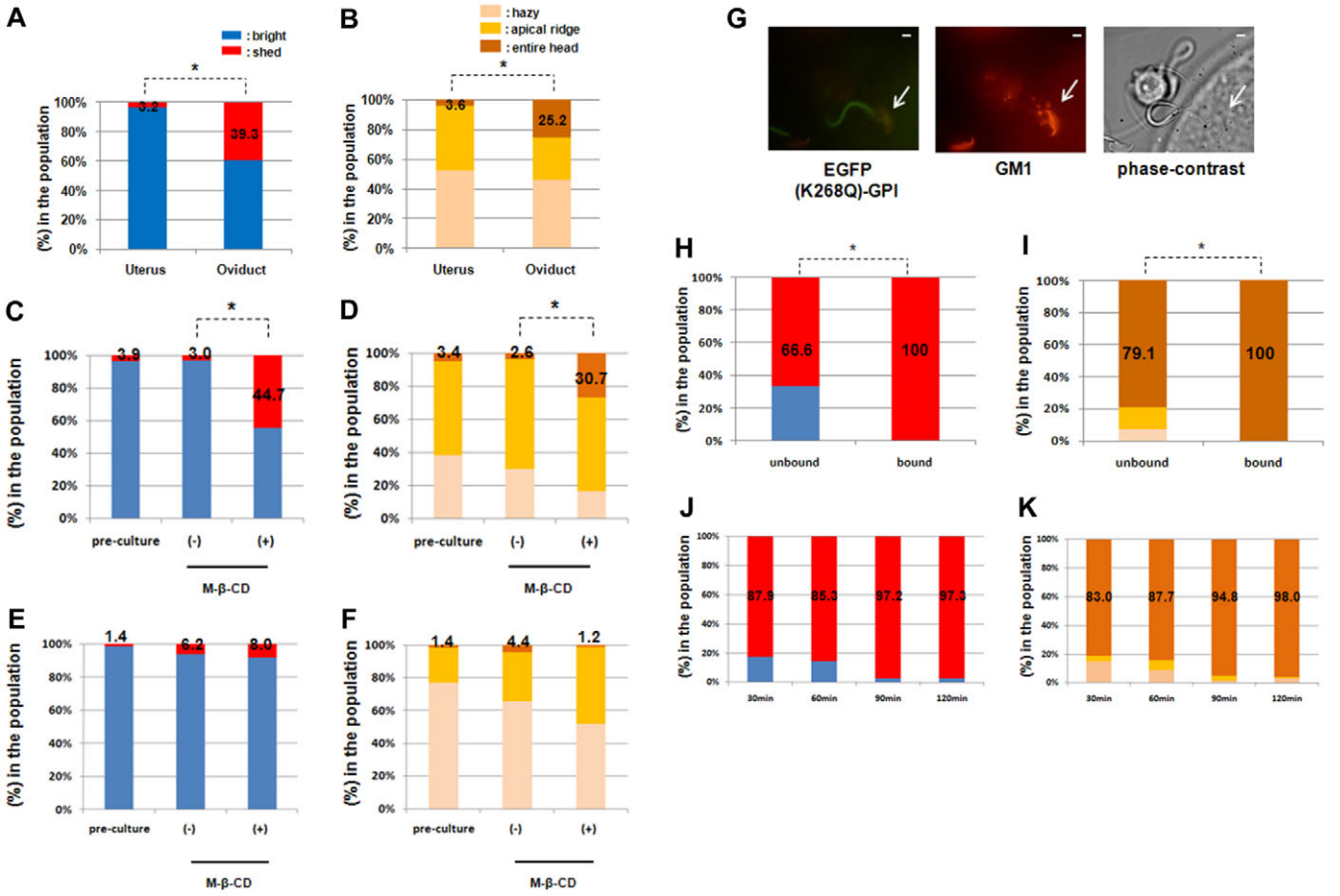

Fig. 6. EGFP (K268Q)-GPI and GM1 status of sperm in vivo. (**A**) EGFP(K268Q)-GPI patterns of ejaculated sperm collected from the uterus and oviduct. Sperm classified with regard to the dual patterns are indicated by their proportion in the population examined. Number of sperm examined: uterus, *n*=93; oviduct, *n*=99. Data from five independent experiments were accumulated. Percentage shed sperm is indicated. (**B**) GM1 staining patterns of sperm collected as in A. Number of sperm examined: uterus, *n*=110; oviduct, *n*=95. Data from three independent experiments were accumulated. Percentage entire head sperm is indicated. (**C**) Incubation of ejaculated sperm collected from the uterus, as described in Fig. 1B, for 30 minutes. Pre-culture, *n*=179; M-β-CD–, *n*=154; M-β-CD+, *n*=170. Data from five independent experiments were accumulated. Percentage shed sperm is indicated. (**D**) GM1 staining patterns of sperm collected as in C. Number of sperm examined: pre-culture, *n*=116; M-β-CD–, *n*=114; M-β-CD+, *n*=114. Data from three independent experiments were accumulated. Percentage entire head sperm is indicated. (**E**) Incubation of ejaculated ACE-deficient sperm carrying EGFP(K268Q)-GPI collected from the uterus, as described in C, for 30 minutes. Number of sperm examined: pre-culture, *n*=139; M-β-CD–, *n*=157; M-β-CD+, *n*=166. Data from three independent experiments were accumulated. Percentage shed sperm is indicated. (**F**) GM1 staining patterns of sperm collected as in E. Number of sperm examined: pre-culture, *n*=139; M-β-CD–, *n*=157; M-β-CD+, *n*=166. Data from three independent experiments were accumulated. Percentage entire head sperm is indicated. (**G**) The ampullae of oviducts were removed from vaginal-plug-positive females. Eggs surrounded by cumulus cells were collected. As seen in the left panel, EGFP(K268Q)-GPI was shed from the sperm head (arrow) and GM1 was apparent in the equatorial pattern (middle panel). Right panel, phase-contrast view. Scale bars: 1 µm. (**H**) EGFP(K268Q)-GPI status of ZP-bound sperm in vivo. Sperm bound or not bound to ZP were examined. Number of sperm examined: unbound, *n*=93; bound, *n*=86. Data from four independent experiments were accumulated. Percentage shed sperm is indicated. (**I**) GM1 staining patterns of sperm collected as in H. Number of sperm examined: unbound, *n*=67; bound, *n*=24. Data from three independent experiments were accumulated. Percentage entire head sperm is indicated. (**J**) Sperm shed of EGFP(K268Q)-GPI during in vitro fertilization. Sperm cultured in HTF-M-β-CD were contacted with unfertilized eggs for the indicated times in HTF-BSA, and then examined. Number of sperm examined: 30 minutes, *n*=174; 60 minutes, *n*=171; 90 minutes, *n*=145; 120 minutes, *n*=150. Data from four independent experiments were accumulated. Percentage shed sperm is indicated. (**K**) GM1 staining patterns during in vitro fertilization. Number of sperm examined: 30 minutes, *n*=130; 60 minutes, *n*=139; 90 minutes, *n*=116; 120 minutes, *n*=100. Data from three independent experiments were accumulated. Percentage entire head sperm is indicated. **P*<0.05 (Student's *t*-test).

and sperm swimming. Because sperm began to swim after warming again up to 37°C, cooling treatment here seemed not to be harmful. All sperm were observed under a fluorescent microscope with a GFP-specific filter system (Olympus). To visualize GM1, Alexa-Fluor-594-conjugated cholera toxin subunit B (CTB, Molecular Probes) was added at the same time. To observe the state of EGFP(K268Q)-GPI in vivo, ejaculated sperm were collected from the uterus or oviducts by flushing with HTF-PVA. 50–70% and more than 90% of sperm were motile in the uterus and oviducts, respectively. To stimulate fertilization condition, M-β-CD was added to the sperm incubations to a final concentration of 0.45 mM.

Calcium ionophore treatment for promoting the acrosome reaction

Epididymal sperm were incubated in HTF-BSA for 2 hours and then further incubated in HTF-BSA containing 10 µM A23187 calcium ionophore (Sigma) for 1 hour.

Immunostaining of Izumo1

Sperm were fixed with 4% neutral buffered formalin, incubated with a rat monoclonal antibody against mouse Izumo1 (Inoue et al., 2008) and then visualized with Alexa-Fluor-488- or Alexa-Fluor-594-conjugated rabbit anti-rat IgG (CTB, Molecular Probes). All sperm were observed under a fluorescent microscope (Olympus).

Journal of Cell Science

In vitro fertilization

Adult C57BL/6J females (more than 10 weeks old) were superovulated by injecting them with 6.7 IU of pregnant mare serum gonadotropin (Teikoku Zoki, Tokyo, Japan) followed 48 hours later with 6.7 IU of human chorionic gonadotropin (Teikoku Zoki). Ovulated eggs surrounded by a cumulus mass were collected from the oviducts 16 hours after the second injection. Eggs with cumuli were incubated in 300 µl of HTF-PVA or HTF-BSA medium, and overlaid with mineral oil. Sperm from the cauda epididymis were preincubated in 200 µl of HTF-PVA, HTF-PVA-M-β-CD, or HTF-BSA for 2 hours and then added to the egg drop at a final concentration of ~1.0×10^5 sperm/ml. Eggs were washed with modified Whitten's medium (mWM; 109.51 mM NaCl, 4.78 mM KCl, 1.19 mM $MgSO_4$, 1.19 mM KH_2PO_4, 22.62 mM $NaHCO_3$, 5.55 mM glucose, 1.49 mM calcium lactate, 0.23 mM sodium pyruvate, 19.1 µg/ml EDTA, 10 µM β-mercaptoethanol, 0.2 mM penicillin G sodium salt, 0.03 mM streptomycin, 3 mg/ml BSA and 0.2 µl of 0.5% phenol red) after 7 hours contact with the sperm, and then incubated in fresh mWM for another 16 hours. To quantify fertilization, the total numbers of unfertilized eggs and two-cell embryos and numbers of two-cell embryos in a population were determined to generate the percentage fertilization value: [(%) fertilization=(number of two-cell embryos/total number of unfertilized eggs and two-cell embryos) ×100]. Values are mean ± s.d.

Sperm-egg binding assay in vivo and in vitro

Adult CD-1 females (more than 10 weeks old) in estrus were mated with EGFP(K268Q)-GPI transgenic males. Twenty hours after the start of mating, ampullae of oviduct were removed from the vaginal-plug-positive females and eggs surrounded by cumulus cells were collected in HTF-PVA supplemented with 10 mM EDTA. For evaluating in vitro sperm–egg binding, sperm cultured in HTF-M-β-CD for 2 hours were inseminated with unfertilized eggs for the indicated times in HTF-BSA. Sperm bound and unbound to the zona pellucida of eggs were stained with Alexa-Fluor-594-conjugated CTB and observed under a fluorescent microscope.

Immunoblotting

Membrane fractions of incubated sperm were prepared using the ProteoExtract™ Native Membrane Protein Extraction kit (EMD Biosciences, La Jolla, CA). After the homogenates and culture supernatants were centrifuged at 25,000 ***g***, the supernatants were collected and assayed for protein content. Next, 10 µg of protein per sample was subjected to SDS-PAGE and then electrophoretically transferred onto a nitrocellulose membrane. The membranes were probed with rabbit polyclonal antibodies against GFP (MBL, Nagoya, Japan), Hyal5 (Kim et al., 2005), Prss21 (Honda et al., 2002), Spam1 (Baba et al., 2002) and Ces3 (generated for this study against peptide, CARNGNPNSEGLPS), or mouse monoclonal antibodies against Adam2, Adam3 (Chemicon International, Temecula, CA) and tACE (Yamaguchi et al., 2006), or a rat monoclonal antibody against mouse Izumo1 (Inoue et al., 2008). Antibody binding was detected and visualized using the ECL Plus system (GE Healthcare Biosciences, Uppsala, Sweden). The blot transfer efficiency was checked by staining with Coomassie Brilliant Blue (Sigma) after immunoblotting. The density of each band was measured by a densitometer and the degree of protein release was calculated as the releasing index in supplementary material Table S2.

Statistical analysis

All data for statistical analyses are displayed in supplementary material Table S3. Differences between two groups were analyzed by Student's *t*-test using Microsoft Excel software. Statistical significance was defined as $*P<0.05$.

We thank Masaru Okabe (Osaka University, Japan) for providing anti-ACE and anti-Izumo1 antibodies, Acrosin-EGFP transgenic mice and helpful discussions, Tadashi Baba (University of Tsukuba, Japan) for anti-Hyal5, anti-Prss21 and anti-Spam1 antibodies and T. Kinoshita for helpful discussions. This work was supported by grants from the Ministry of Education, Science, Sports and Culture of Japan and the Fujiwara Foundation.

Supplementary material available online at
http://jcs.biologists.org/cgi/content/full/124/15/2573/DC1

References

Baba, D., Kashiwabara, S., Honda, A., Yamagata, K., Wu, Q., Ikawa, M., Okabe, M. and Baba, T. (2002). Mouse sperm lacking cell surface hyaluronidase PH-20 can pass through the layer of cumulus cells and fertilize the egg. *J. Biol. Chem.* **277**, 30310-30314.

Baibakov, B., Gauthier, L., Talbot, P., Rankin, T. L. and Dean, J. (2007). Sperm binding to the zona pellucid is not sufficient to induce acrosome exocytosis. *Development* **134**, 933-943.

Bailey, J. L. (2010). Factors regulating sperm capacitation. *Syst. Biol. Reprod. Med.* **56**, 334-348.

Buttke, D. E., Nelson, J. L., Schlegel, P. N., Hunnicutt, G. R. and Travis, A. J. (2006).Visualization of GM1 with cholera toxin B in live epididymal versus ejaculated bull, mouse, and human spermatozoa. *Biol. Reprod.* **74**, 889-895.

Clark, G. F. and Dell, A. (2006). Molecular models for murine sperm-egg binding. *J. Biol. Chem.* **281**, 13853-13856.

Costello, S., Michelangeli, F., Nash, K., Lefievre, L., Morris, J., Machado-Oliveria, G., Barratt, C., Kirkman-Brown, J. and Publicover, S. (2009). Ca^{2+}-stores in sperm: their identities and functions. *Reproduction* **138**, 425-437.

Davis, B. K. (1981). Timing of fertilization in mammals: sperm cholesterol/phospholipid ratio as a determinant of the capacitation interval. *Proc. Natl. Acad. Sci. USA* **78**, 7560-7564.

Deguchi, E., Tani, T., Watanabe, H., Yamada, S. and Kondoh, G. (2007). Dipeptidase-inactivated tACE action in vivo: selective inhibition of sperm-zona pellucida binding in the mouse. *Biol. Reprod.* **77**, 794-802.

Fuchs, S., Frenzel, L., Hubert, C., Lyng, R., Muller, L., Michaud, A., Xiao, H. D., Adams, J. W., Capecchi, M. R., Corvol, P. et al. (2005). Male fertility is dependent on dipeptidase activity of testis ACE. *Nat. Med.* **11**, 1140-1142.

Fujiwara, Y., Murakami, M., Inoue, N., Satouh, Y., Kaseda, K., Ikawa, M. and Okabe, M. (2010). Sperm equatorial segment protein 1, SPESP1, is required fully fertile sperm in mouse. *J. Cell Sci.* **123**, 1531-1536.

Hagaman, J. R., Moyer, J. S., Bachman, E. S., Sibony, M., Magyar, P. L., Welch, J. E., Smithies, O., Krege, J. H. and O'Brien, D. A. (1998). Angiotensin-converting enzyme and male fertility. *Proc. Natl. Acad. Sci. USA* **95**, 2552-2557.

Honda, A., Yamagata, K., Sugiura, S., Watanabe, K. and Baba, T. (2002). A mouse serine protease TESP5 is selectively included into lipid rafts of sperm membrane presumably as a glycosylphosphatidylinositol-anchored protein. *J. Biol. Chem.* **277**, 16976-16984.

Ikawa, M., Inoue, N., Benham, A. M. and Okabe, M. (2010). Fertilization: a sperm's journey to and interaction with the oocyte. *J. Clin. Invest.* **120**, 984-994.

Inoue, N., Ikawa, M., Isotani, A. and Okabe, M. (2005). The immunoglobulin superfamily protein Izumo is required for sperm to fuse with eggs. *Nature* **434**, 234-238.

Inoue, N., Ikawa, M. and Okabe, M. (2008). Putative sperm fusion protein IZUMO and the role of N-glycosylation. *Biochem. Biophys. Res. Commun.* **377**, 910-914.

Jacobson, K., Mouritsen, O. G. and Anderson, R. G. W. (2007). Lipid rafts: at a crossroad between cell biology and physics. *Nat. Cell Biol.* **9**, 7-14.

Jones, R., Howes, E., Dunne, P. D., James, P., Bruckbauer, A. and Klernerman, D. (2010). Tracking diffusion of GM1 gangliosides and zona pellucid binding molecules in sperm plasma membranes following cholesterol efflux. *Dev. Biol.* **339**, 398-406.

Kim, E., Baba, D., Kimura, M., Yamashita, M., Kashiwabara, S. and Baba, T. (2005). Identification of a hyaluronidase, Hyal5, involved in penetration of mouse sperm through cumulus mass. *Proc. Natl. Acad. Sci. USA* **102**, 18028-18033.

Kondoh, G. (2002). Development of glycosylphosphatidylinositol-anchored enhanced green fluorescent protein. Green fluorescent protein: applications and protocols. *Methods Mol. Biol.* **183**, 215-224.

Kondoh, G., Gao, X. H., Nakano, Y., Koike, H., Yamada, S., Okabe, M. and Takeda, J. (1999). Tissue-inherent fate of GPI revealed by GPI-anchored GFP transgenesis. *FEBS Lett.* **458**, 299-303.

Kondoh, G., Tojo, H., Nakatani, Y., Komazawa, N., Murata, C., Yamagata, K., Maeda, Y., Kinoshita, T., Okabe, M., Taguchi, R. and Takeda, J. (2005). Angiotensin-converting enzyme is a GPI-anchored protein releasing factor crucial for fertilization. *Nat. Med.* **11**, 160-166.

Kondoh, G., Watanabe, H., Tashima, Y., Maeda, Y. and Kinoshita, T. (2009). Testicular angiotensin-converting enzyme with different glycan modification: characterization on glycosylphosphatidylinositol-anchored protein releasing and dipeptidase activities. *J. Biochem.* **145**, 115-121.

Mishra, S. and Joshi, P. G. (2007). Lipid raft heterogeneity: an enigma. *J. Neurochem.* **103**, 135-142.

Nakanishi, T., Ikawa, M., Yamada, S., Parvinen, M., Baba, T., Nishimune, Y. and Okabe, M. (1999). Real-time observation of acrosomal dispersal from mouse sperm using GFP as a marker protein. *FEBS Lett.* **449**, 277-283.

Niwa, H., Yamamura, K. and Miyazaki, J. (1991). Efficient selection for high-expression transfectants with a novel eukaryotic vector. *Gene* **108**, 193-199.

Nixon, B., Bielanowicz, A., McLaughlin, E. A., Tanphaichitr, N., Ensslin, M. A. and Aitken, R. J. (2008). Composition and significance of detergent resistant membranes in mouse spermatozoa. *J. Cell. Physiol.* **218**, 122-134.

Okabe, M., Adachi, T., Takada, K., Oda, H., Yagasaki, M., Kohama, Y. and Mimura, T. (1987). Capacitation-related changes in antigen distribution on mouse sperm heads and its relation to fertilization rate in vitro. *J. Reprod. Immunol.* **11**, 91-100.

Selvaraj, V., Buttke, D., Asano, A., Mcelwee, J. L., Wolff, C. A., Nelson, J. L., Klaus, A. V., Hunnicutt, G. R. and Travis, A. J. (2007). GM1 dynamics as a marker for membrane changes associated with the process of capacitation in murine and bovine spermatozoa. *J. Androl.* **28**, 588-599.

Shum, W. W., Da Silva, N., McKee, M., Smith, P. J., Brown, D. and Breton, S. (2008). Transepithelial projections from basal cells are luminal sensors in pseudostratified epithelia. *Cell* **135**, 1108-1117.

Simons, K. and Toomre, D. (2000). Lipid rafts and signal transduction. *Nat. Rev. Cell Biol.* **1**, 31-39.

Smith, T. T. and Yanagimachi, R. (1990). The viability of hamster spermatozoa stored in the isthmus of the oviduct: the importance of sperm-epithelium contact for sperm survival. *Biol. Reprod.* **42**, 450-457.

Suarez, S. S. (2008). Control of hyperactivation in sperm. *Hum. Reprod. Update* **14**, 647-657.

Sullivan, R., Saez, F., Girouard, J. and Frenette, G. (2005). Role of exosomes in sperm maturation during the transit along the male reproductive tract. *Blood Cells Mol. Dis.* **35**, 1-10.

Takeo, T., Hoshii, T., Kondo, Y., Toyodome, H., Arima, H., Yamamura, K.-I., Irie, T. and Nakagata, N. (2008). Methyl-beta-cyclodextrin improves fertilizing ability of

C57BL/6 mouse sperm after freezing and thawing by facilitating cholesterol efflux from the cells. *Biol. Reprod.* **78**, 546-551

Travis, A. J. and Kopf, G. S. (2002). The role of cholesterol efflux in regulating the fertilization potential of mammalian spermatozoa. *J. Clin. Invest.* **110**, 731-736.

Ueda, Y., Yamaguchi, R., Ikawa, M., Okabe, M., Morii, E., Maeda, Y. and Kinoshita, T. (2007). PGAP1 knock-out mice show otocephaly and male infertility. *J. Biol. Chem.* **282**, 30373-30380.

Varma, R. and Mayor, S. (1998). GPI-anchored proteins are organized in submicron domains at the cell surface. *Nature* **394**, 798-801.

Visconti, P. E., Bailey, J. L., Moore, G. D., Pan, D., Olds-Clarke, P. and Kopf, G. S. (1995). Capacitation of mouse spermatozoa. I. Correlation between the capacitation state and protein tyrosine phosphrylation. *Development* **121**, 1129-1137.

Visconti, P. E., Galantino-Homer, H., Ning, X., Moore, G. D., Valenzuela, J. P., Jorgez, C. J. and Alvarez, J. G. and Kopf, G. S. (1999). Cholesterol-efflux mediated signal transduction in mammalian sperm. β-cyclodextrins initiate transmembrane signaling leading to an increase in protein tyrosine phosphorylation and capacitation. *J. Biol. Chem.* **274**, 3235-3242.

Wassarman, P. M. and Litscher, E. S. (2001). Towards the molecular basis of sperm and egg interaction during mammalian fertilization. *Cells Tissues Organs* **168**, 36-45.

Wassarman, P. M. and Litscher, E. S. (2008). Mammalian fertilization is dependent on multiple membrane fusion events. *Methods Mol. Biol.* **475**, 99-113.

Yamaguchi, R., Yamagata, K., Ikawa, M., Moss, S. B. and Okabe, M. (2006). Aberrant distribution of ADAM3 in sperm from both angiotensin-converting enzyme (ACE)-deficient and calmegin (Clgn)-deficient mice. *Biol. Reprod.* **75**, 760-766.

Yanagimachi, R. (1988). Mammalian fertilization. In *The Physiology of Reproduction* Vol. 1 (ed. E. Knobil and J. D. Neil), pp. 135-173. New York: Raven Press.

Yanagimachi, R. (2009). Germ cell research: a personal perspective. *Biol. Reprod.* **80**, 204-218.

Journal of Cell Science